JOURNAL OF GEOPHYSICAL RESEARCH: EARTH SURFACE, VOL. 118, 42–53, doi:10.1029/2012JF002354, 2013

Entrainment of coarse particles in turbulent flows: An energy approach

Manousos Valyrakis,[1] Panayiotis Diplas,[2] and Clint L. Dancey[3]

Received 25 January 2012; revised 21 November 2012; accepted 22 November 2012; published 25 January 2013.

[1] The entrainment of coarse sediment particles under the action of fluctuating hydrodynamic forces is investigated from an energy perspective. It is demonstrated that the entrainment of a grain resting on the channel boundary is possible when the instantaneous flow power transferred to it exceeds a critical level. Its complete removal from the bed matrix occurs only if the impinging flow events supply sufficient mechanical energy. The energy-based criterion is formulated theoretically for entrainment of individual spherical particles in both saltation and rolling modes. Out of the wide range of flow events that can perform mechanical work on a coarse grain, only those with sufficient power and duration or equivalent energy density and characteristic length scale may accomplish its complete dislodgement. The instantaneous velocity upstream of a mobile particle is synchronously recorded with its position, enabling the identification of the flow events responsible for grain entrainment by rolling at near incipient motion flow conditions. For each of the entrainment events, the energy transfer coefficient defined as the ratio of the mechanical work performed on the particle to the mean energy of the flow event responsible for its dislodgement obtains values ranging from 0.04 to 0.10. At the examined low-mobility flow conditions, the majority (about 80%) of the energetic structures leading to complete particle entrainment have a characteristic length of about two to four particle diameters.

Citation: Valyrakis, M., P. Diplas, and C. L. Dancey (2013), Entrainment of coarse particles in turbulent flows: An energy approach, *J. Geophys. Res. Earth Surf.*, *118*, 42–53, doi:10.1029/2012JF002354.

1. Introduction

[2] Sediment transport in rivers, estuaries, and aeolian environments represents one of the major challenges to engineers and researchers in the field of earth surface dynamics. Of specific interest is the accurate identification of the flow conditions near the threshold of movement. This has a wide range of applications from stable channel design to establishing acceptable flushing flow rates downstream of reservoirs.

[3] A number of diverse theories have been proposed in an attempt to relate flow strength, expressed by means of a certain flow parameter or derivatives of it, to the resulting rates of sediment transport. These theories can be classified into two basic categories, depending on the fundamental laws of physics they rely on.

[4] The first approach, based on Newton's laws of motion, uses vectorial quantities such as mean stream velocity (U) [*Hjulström*, 1939] or *Shields*'s [1936] parameter, $\tau^* = \tau/[g(\rho_s - \rho_f)D_{50}]$ (where τ is the boundary shear stress, g the acceleration of gravity, D_{50} the bed material median size, and ρ_f and ρ_s the density of fluid and sediment, respectively). This approach is widely used for identifying flow conditions near incipient movement despite the criticism it has received in the literature [*Miller et al*., 1977; *Bettess*, 1984; *Buffington and Montgomery*, 1997; *Shvidchenko and Pender*, 2000; *Paphitis et al*., 2002].

[5] The second approach is linked to the laws of thermodynamics, trying to correlate the scalar variables of energy or its derivative quantities to the rate of entrainment of sediment. One of the first attempts to emphasize the role of "stream energy" on sediment discharge can be found in the classical work of *Gilbert* [1914]. Gilbert specified that the rate of expenditure of available potential energy between two stations of different elevation equals the product QSg, with Q the water discharge and S the bed slope. Since then, power theories have been related to the rate of expenditure of kinetic energy of the stream or of available potential energy (gravitational power) to transport sediment by a number of researchers [*Rubey*, 1933; *Knapp*, 1938; *Bagnold*, 1956]. However, it was not until the work of *Bagnold* [1966] that this concept was extended to develop quantitative equations for the prediction of total sediment concentration. *Bagnold* [1966] introduced the concept of specific stream power, $\omega = Q\,Sg/b$, with b the width or hydraulic perimeter of the stream, as the

[1]Infrastructure and Environment Research Division, School of Engineering, University of Glasgow, Glasgow G12 8LT, UK.
[2]Baker Environmental Hydraulics Laboratory, Department of Civil and Environmental Engineering, Virginia Tech, Blacksburg, Virginia, USA.
[3]Baker Environmental Hydraulics Laboratory, Department of Mechanical Engineering, Virginia Tech, Blacksburg, Virginia, USA.

Corresponding author: M. Valyrakis, Infrastructure and Environment Research Division, School of Engineering, University of Glasgow, Room 735 Rankine Building, Oakfield Avenue, Glasgow G12 8LT, UK. (manousos.valyrakis@glasgow.ac.uk)

2169-9003/13/2012JF002354

rate of the stream's energy supply per unit area or simply as the product $U\tau$ [*Bagnold*, 1977, 1980, 1986]. *Yang* [1972] hypothesized that unit stream power, defined as the rate of expenditure of potential energy per unit weight of water and given by the product of mean flow velocity and energy slope, US, is the pertinent quantity controlling the concentration of suspended sediment, bed load, or total sediment discharge as verified from statistical analysis of experimental data [*Yang*, 1972, 1979; *Yang and Stall*, 1976; *Yang and Molinas*, 1982].

[6] Both traction and power approaches usually use temporally and sometimes spatially averaged quantities such as mean velocity, bed shear stress, or their product. Such mean quantities fail to capture the effect of rapidly fluctuating hydrodynamic forces on the entrainment of bed material. Particularly for the rough turbulent flow regime (e.g., boundary Reynolds number, $\boldsymbol{R}_* = [u_* D_{50}/\nu] > 100$, with u_* the shear velocity, and ν the kinematic viscosity of water), Shields's criterion for inception of motion of coarse particles shows scatter of more than an order of magnitude [e.g., *Buffington and Montgomery*, 1997; *Lavelle and Mofjeld*, 1987]. Many researchers acknowledging the limitations of the above criteria, particularly for near-critical flow conditions, have emphasized the significance of the magnitude of peaks in the instantaneous hydrodynamic forces in the vicinity of the boundary [*Einstein and El-Samni*, 1949; *Sutherland*, 1967; *Paintal*, 1971; *Apperley and Raudkivi*, 1989; *Papanicolaou et al*., 2001; *Sumer et al*., 2003; *Zanke*, 2003; *Hofland et al*., 2005; *Schmeeckle et al*., 2007; *Vollmer and Kleinhans*, 2007; *Dwivedi et al*., 2010, 2011b]. Recently, *Diplas et al*. [2008] demonstrated the importance of duration of flow events above a critical level of the instantaneous stress tensor and suggested their product, impulse, as the criterion to characterize incipient motion conditions. *Valyrakis et al*. [2010] extended the proposed impulse criterion over a wide range of grain mobility levels for both saltating and rolling particles. The validity of the impulse concept and the results of the theoretical formulation were demonstrated through a series of appropriately designed experiments [*Diplas et al*., 2008; *Valyrakis et al*., 2010].

[7] In this study, a new criterion for particle entrainment linking the available energy of turbulent flow events to the mechanical work required for grain entrainment is proposed for both pure saltation and rolling. The energy approach to grain dislodgement, although directly linked to the impulse criterion, is demonstrated to be more versatile and intuitive. The validity of the proposed criterion is examined through the detailed analysis of data obtained from flume experiments corresponding to low-mobility conditions.

2. Role of Energetic Events on Grain Entrainment

[8] Customarily theoretical deterministic or stochastic studies of inception of motion of grains from the bed matrix have implemented a force and moments balance approach for both saltation [*Cheng and Chiew*, 1998; *Wu and Lin*, 2002] and rolling entrainment modes [*Papanicolaou et al*., 2002], respectively. Specifically, such traditional approaches define that entrainment occurs when the drag and lift forces, commonly parameterized by the square of the instantaneous local flow velocity, $u_f(\mathrm{t})^2$, in the vicinity of the particle [e.g., *Einstein and El-Samni*, 1949; *White*, 1940], exceed a critical level (u_c^2) that may be determined from the particle properties and the local grain configuration [e.g., *Valyrakis et al*., 2010].

[9] From an energy viewpoint, the temporal history of the instantaneous flow power defined as a linear function of the cube of local flow velocity, $P_f(t) = \mathrm{f}(u_f(\mathrm{t})^3)$, is of interest rather than the instantaneous hydrodynamic forces or stresses. Then the condition $u_f(\mathrm{t}) > u_c$, describes when the transfer of flow energy to the particle is positive. For such cases, the available flow power is linked to the rate of energy transferred from the flow to the particle via the relationship $C_{eff}\ P_f = \Delta W_p\ /\Delta t$, where $C_{eff} = u_p/u_f$ is the mean energy transfer coefficient, u_p and u_f are the particle and flow velocities (averaged over the time interval Δt), and ΔW_p is the mechanical work done on the particle over Δt. Thus, peaks in the temporal history of the instantaneous $P_f(t)$ have a potential to perform work on the particle by setting it into motion.

[10] However, the above condition does not suffice to guarantee complete entrainment, as demonstrated by the following example obtained from laboratory experiments. A portion of the temporal history of $u_f(t)^3$ measured in the vicinity (i.e., one particle diameter upstream) of an exposed particle along with the instance of its complete entrainment (dotted vertical line) are shown in Figure 1. Based on the condition $u_f(t) > u_c$, two flow events have the potential to entrain the particle (events A and B in Figure 1). It is observed that complete dislodgement does not occur with the flow event having the greater instantaneous peak of P_f. On the contrary, the later flow event (B), lasting significantly longer ($T_B > T_A$), is capable of completely dislodging the particle out of its pocket. It is concluded that the rate of flow energy transfer is an important indicator signifying the local strength of flow toward grain mobilization, but alone it does not suffice to determine which of the flow events may trigger a complete grain entrainment.

[11] A quantity, which accounts for both the local power of flow, $P_f(t)$, and the duration (T_i) of a flow event i over which mechanical work is performed toward particle entrainment, is the available energy of the flow event, defined as the following integral:

$$E_{f,i} = \int_{t_0}^{t_0+T_i} P_f(t)dt, \text{with } u_f(t) > u_c \text{ for } \mathrm{t}_0 < t < t_0 + T_i \quad (1)$$

where t_0 refers to the time instant when the flow event commences transferring energy to the grain. A suitable criterion for specifying the threshold level for grain entrainment should link the amount of energy transferred by energetic flow events, $C_{eff}E_{f,i}$, with the minimum amount of work required for particle entrainment, $W_{p,cr}$:

$$C_{eff}E_{f,i} > W_{p,cr} \quad (2)$$

[12] According to the event-based energy balance framework presented in equation (2), if the duration of the energetic event or the length scale of the flow structure is long enough to transfer sufficient mechanical energy to the grain, then full grain entrainment is possible. In this manner, the dynamic significance of the fluctuating near-boundary velocity and pressure fields in transferring energy to mobilize sediment grains is accounted for by considering the short but

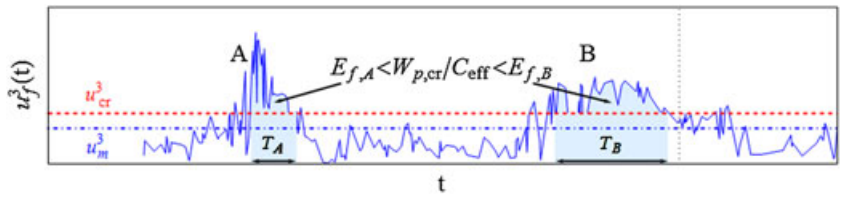

Figure 1. Schematic of the time history of instantaneous flow power ($P_f \sim u_f^3$) exerted on a completely exposed particle. Energetic flow events (E_i, shaded areas) have instantaneous flow power in excess of the threshold level (u_{cr}^3, dashed line) lasting for duration (T_i). The duration of the energetic flow events is of the order of 10 ms. The flow conditions are subthreshold, as shown by a mean velocity level below critical, $u_m < u_{cr}$. The instant of full entrainment is denoted by the dotted vertical line.

finite duration of energetic flow events. For the example of Figure 1, the applicability of the energy criterion may be demonstrated by comparing the shaded areas $E_{f,A}$ and $E_{f,B}$, which represent the portion of flow energy made available for mobilizing the grain. The amount of flow energy required for full grain entrainment, $W_{p,cr}$, should lie between the energy values of the events resulting in full dislodgement and those that do not ($E_{f,A} < W_{p,cr}/C_{eff} < E_{f,B}$).

[13] In the following, the above conjecture is investigated by providing the theoretical framework for two modes of entrainment, namely, saltation and rolling. Data from a series of flume experiments near incipient motion conditions are analyzed to further demonstrate the validity and utility of the energy concept.

3. Energy Criterion Formulation

[14] Two modes of grain dislodgement are considered in this study: saltation and rolling. The frequency of occurrence of each entrainment mode strongly relates to different dynamic processes and specific bed microtopographies. For instance, a completely hidden grain resting on the bed surface layer experiences lift forces, F_L, that may cause its saltation (Figure 2a). On the contrary, a grain with maximum exposure to the approaching flow experiences hydrodynamic drag forces, F_D, which usually trigger its movement (Figure 2b). Consistent with the dynamic definition of grain entrainment [*Valyrakis et al.*, 2010], a particle is considered to have enough energy to perform a complete entrainment when it can reach a new location of higher elevation or greater exposure from where its further dislodgement downstream is guaranteed. Thus, the work that needs to be performed ($W_{p,cr}$) for complete grain removal should equal the change in potential energy between the location it has to be raised and its resting position. This critical level depends only on particle properties and local grain arrangement characteristics, being proportional to the elevation difference between the two positions.

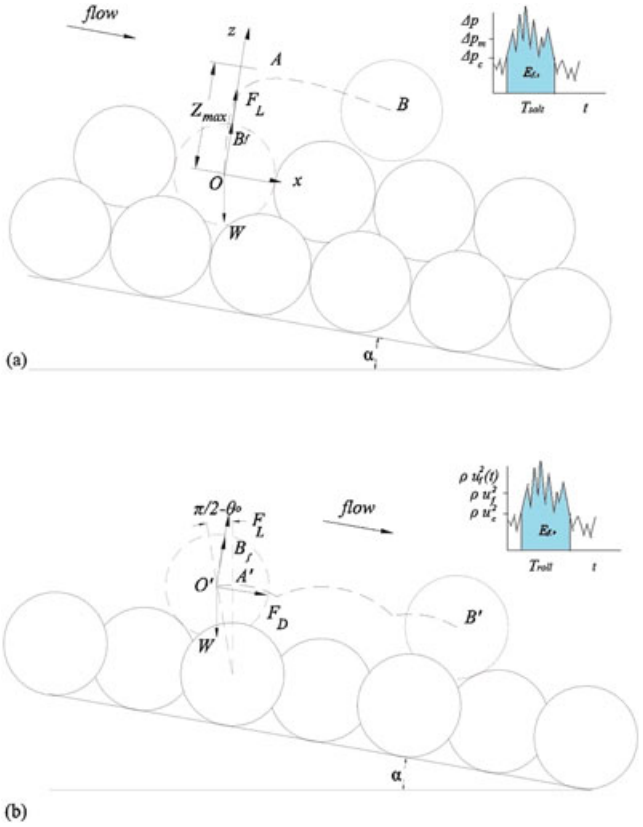

Figure 2. Entrainment of particle by: (a) saltation, mobile particle (dashed circle) is initially surrounded by neighboring particles; and (b) rolling, mobile particle (dashed circle) is completely exposed to the flow. For both cases, the position of the downstream entrained particle, due to mean flow forcing, is depicted with a continuous thick circle, whereas the path followed is shown with a dotted-dashed curve. Complete entrainment is initiated by energetic events above critical, $E_{f,i}$, shown in the inset.

3.1. Incipient Saltation

[15] The entrainment of coarse grains by saltation, due to the action of hydrodynamic lift forces, has been the focus of many theoretical and experimental studies [*Jeffreys*, 1929; *Chepil*, 1958; *Benedict and Christensen*, 1972; *Cheng and Chiew*, 1998; *Wu and Lin*, 2002; *Nino et al.*, 2003; *Dwivedi et al.*, 2011a]. The representative case of hexagonal arrangement of spherical particles comprising a fully packed bed surface is shown in Figure 2a. For such a local configuration, a particle may be initially entrained, when the pressure difference between its top and bottom surfaces (Δp) is significant (resulting in a mean lift force greater than the submerged particle weight) and then follow a projectile-like motion (similar to trajectory *OAB*, Figure 2a) due to the mean flow forcing. Typically, the theoretical development of a criterion for inception of saltation is based on balance of the

hydrodynamic lift force (F_L), the buoyancy, $B_f=\rho_f Vg\cos\alpha$, with α the bed slope, $V=4\pi R_m^3/3$ the grain volume and R_m its radius, and the particle weight, $W=\rho_s Vg$. However, here, an energy (rather than a force) balance equation is used (equation (2)).

[16] According to equation (2), energy is supplied to a solid particle from an impinging energetic flow event ($E_{f,i}$) of characteristic size and energy density. The maximum area over which the flow structure transfers energy to a particle is effectively limited by the cross-sectional area of the latter perpendicular to the flow direction, $A=\pi R_m^2$. This flow structure has a characteristic stream-wise length scale that may be defined as the product of its mean advection velocity (u_f) and duration (T_{salt}). The pressure difference between the top and bottom surface of the particle, Δp_m, averaged over the duration of the flow event may be considered as a representation of the mean energy density of the flow structure due to the rapidly fluctuating pressure field. *Einstein and El-Samni* [1949] performed a series of experiments to directly relate the pressure difference between the upper and lower surface of hemispheres fixed to the wall with the velocity measured 0.35 diameter from the theoretical bed level. Based on their findings, the mean value of energy density can be related to the average velocity of the flow event:

$$\Delta p_m = C_p \rho_f u_f^2 \tag{3}$$

with C_p a mean pressure coefficient. Equation (3) may be thought as an expression for the energy density ($C_p\rho_f u_f^2$) of the flow event. The overall impact of the flow event with regard to particle entrainment depends on the characteristic dimensions of this flow event, namely, its stream-wise length ($u_f\ T_{\text{salt}}$) and the effective area of its interaction with the solid particle ($C_A A$, with $C_A(<1)$ an effectiveness coefficient denoting the percentage of the particle's cross-sectional area over which the flow forcing is applied). Then the available flow energy for saltation, $E_{f,s}$, may be defined as the product:

$$E_{f,s} = \left(u_f T_{salt}\right)\left(C_A A\right)\left(C_p \rho_f u_f^2\right) \tag{4}$$

[17] The particle should be able to reach the topmost position ($z_{\max}$) with the energy supplied from the flow event. Then the work performed on the particle during the advection of the flow structure should match the minimum mechanical energy at this location or equally the stored potential energy:

$$W_{p,s} = \left(\rho_s - \rho_f\right) cos\alpha\ Vg\ z_{\max} \tag{5}$$

[18] For threshold conditions, the required particle displacement may be considered of the order of its diameter ($z_{\max}=2R_m$). Consequently, the energy equation (2) becomes for the case of a saltating grain:

$$\left(C_{salt} u_f T_{salt}\right)\left(C_A C_p u_f^2\right) \geq \frac{8}{3}\cos\alpha \frac{\rho_s - \rho_f}{\rho_f} g R_m^2 \tag{6}$$

with C_{salt} ($=u_p/u_f$) denoting the efficiency of flow energy transfer to the saltating grain. Equation (6) suggests that the flow energy per unit area of the particle transferred toward its entrainment remains constant. It also demonstrates the dependence of the proposed criterion on particle and bed properties, while identifying the characteristics of the energetic flow events relevant to grain mobilization, which may be expressed in terms of the threshold curves. In particular, threshold energy levels may be expressed as a combination of average effective power of the flow event (P_f) and its duration (T_{salt}), or equivalently its specific energy ($\Delta p_m/\rho_f$) and characteristic advection length scale ($u_f \cdot T_{\text{salt}}$), varying in an inversely proportional manner.

[19] An illustrative example is provided in Figures 3a and 3b, where the threshold curve is expressed in terms of the above quantities. The threshold curve is predicted from the energy equation for saltation, for the case of a 12.7 mm spherical particle resting on a horizontal layer of a closely packed arrangement of the same particles with density $\rho_s-\rho_f=1300\,\text{kg/m}^3$, in water (similar to Figure 2a). Flow events defining points that fall above the hyperbolic-shaped curve (Figures 3a and 3b) will result in particle removal from its resting configuration, whereas those below the curve will not suffice for complete particle dislodgement.

[20] Extreme pressure events are short-lived, and depending on the flow conditions and bed, configuration may reach even more than six times the time mean value [*Hofland et al*., 2005; *Schmeeckle et al*., 2007]. Despite their variability, the energy criterion captures the essential characteristics of energetic flow structures leading to entrainment. For instance, a flow event of magnitude $6\Delta p/\rho_f$ and duration ΔT results in the same particle response as a flow event with smaller peak ($3.8\Delta p/\rho_f$) and twice as long the duration ($2\Delta T$), based on equation (6). These results are consistent to those derived from the impulse concept [*Diplas et al*., 2008; *Valyrakis et al*., 2010] for saltating particles and short T. More specifically, it may be shown that the two criteria are fundamentally connected to

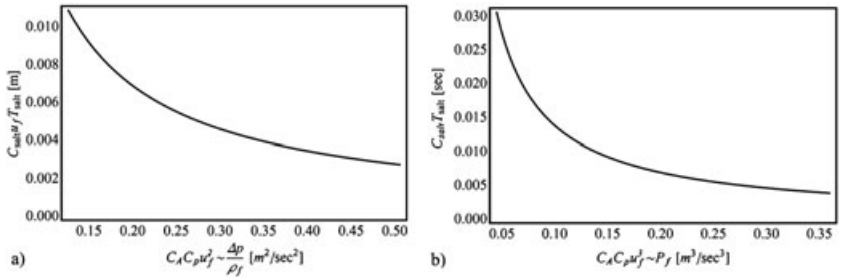

Figure 3. Representation of energy threshold for entrainment of a 12.6 mm particle in saltation mode by: (a) mean specific energy and advection length scale, and (b) mean flow power (P_f) and duration ($C_{\text{salt}}T_{\text{salt}}$) combinations.

each other using the energy-impulse equation, $W_{p,s}=I_{\text{salt}}\cdot u_p$, with $I_{\text{salt}}=F_L T_{\text{salt}}$, the critical impulse required for particle entrainment in saltation mode (cf. equation (7), in [*Valyrakis et al*., 2010]).

3.2. Incipient Rolling

[21] The development of an energy-based criterion for the entrainment of coarse grains by rolling mode follows the same rationale used for the derivation of the energy threshold for saltation. While a grain hidden in the surface layer is mobilized by lift forces, in the limiting case of a fully exposed particle, entrainment is the outcome of mechanical work performed by the action of hydrodynamic drag (F_D). Usually, for unobstructed uniform flows, the rapidly fluctuating lift forces (F_L) have a rather secondary role in facilitating grain removal [*Zanke*, 2003; *Hofland et al*., 2005; *Schmeeckle et al*., 2007]. Depending on the flow conditions and particle arrangement, the effect of F_L may be taken into account by appropriately adjusting the particle weight (and effectively $W_{p,cr}$) or simply be neglected. In contrast to past theoretical approaches using balance of moments of forces and applied torques about an axis of rotation or a pivot point [*White*, 1940; *Komar and Li*, 1988; *James*, 1990; *Wu and Yang*, 2004], an event-based energy balance framework is used in this study.

[22] A spherical particle resting on top of similar bed grains fully dislodges when it reaches the topmost position of the local bed arrangement (location A' in Figure 2b). From this location of maximum exposure, the particle may further be transported downstream by the action of the mean flow (e.g., follow the path $O'A'B'$, Figure 2b). The work performed on the particle for rolling ($W_{p,r}$), will depend on the required angular displacement $\theta=\pi/2-\theta_0$, with θ_0, the pivoting angle, formed between the horizontal and the lever arm (L_{arm}):

$$W_{p,r} = \left(\rho_s-\rho_f\right)\cos\alpha V g(1-\sin\theta_0)L_{arm} \tag{7}$$

[23] The flow energy transferred during the passage of a sufficiently energetic flow structure should equal or exceed the mechanical work, $W_{p,r}$. Such flow events apply high normal and shear stresses to the particle transferring flow energy at a rate proportional to the cube of the instantaneous approaching flow velocity, for duration T_{roll} equal to the time required for the advection of the flow event. Similar to the case of entrainment by saltation, the available energy of the flow event for rolling, $E_{f,r}$, may be given as the product of the energy density of the flow structure $[(C_D/2)\rho_f u_f^2]$, its stream-wise length ($u_f T_{roll}$), and the portion of the exposed area of the solid particle ($C_A A$):

$$E_{f,r} = (C_A A)\left(\frac{C_D}{2}\rho_f u_f^2\right)\left(u_f T_{roll}\right) \tag{8}$$

[24] Incorporating the efficiency of flow energy supply to the rolling grain with the energy transport coefficient for rolling mode ($C_{roll}=u_p/u_f$), equations (2), (7), and (8) yield:

$$\left(C_{roll}u_f T_{roll}\right)\left(\frac{C_D}{2}C_A u_f^2\right)\geq\frac{4}{3}\cos\alpha(1-\sin\theta_0)\frac{\rho_s-\rho_f}{\rho_f}gL_{arm}R_m \tag{9}$$

[25] In addition to the particle's properties such as its radius (R_m) and density (ρ_s), equation (9) indicates the dependence of the threshold on the local microtopography parameters such as the lever arm [$L_{\text{arm}}=(2R_m{}^2+8R_mR_b)^{1/2}$, with R_b the radius of particles forming the surface layer] and pivot angle $\{\theta_0=\alpha+\text{arc}cot[R_b/(3R_m^2+6R_mR_b-R_b^2)]\}$. With regard to the features of the flow events mobilizing the particle, it is noticed that the mean magnitude of their energy density is linked to its length scale in an inverse fashion. Similarly, the longer the flow structure transfers energy to the particle, the less the magnitude of required power; likewise, the greater the rate of energy supply is, the shorter the minimum duration required for particle dislodgement will be.

[26] For instance, a quantitative example may be offered, considering the spherical particle (R_m=6.35 mm, $\rho_s-\rho_f$= 1300 kg/m^3), shown in Figure 2b, entrained in water by rolling. The critical energy level predicted from the energy equation for rolling (equation (9)), using the equal sign) is illustrated (thick curve in Figures 4a and 4b). The qualitative dependence of the magnitude of the event in terms of energy density or power and its scale expressed in stream-wise length size or duration, shown in Figures 4a and 4b, respectively, are similar to the case of saltation. Only the events represented by points above the predicted threshold curve may transfer enough flow energy for full entrainment.

[27] The energy criterion for rolling is directly related to the corresponding impulse criterion via the energy-impulse equation $W_{p,r}=I_{roll}\cdot u_p$, with $I_{roll}=F_D T_{roll}$, the critical

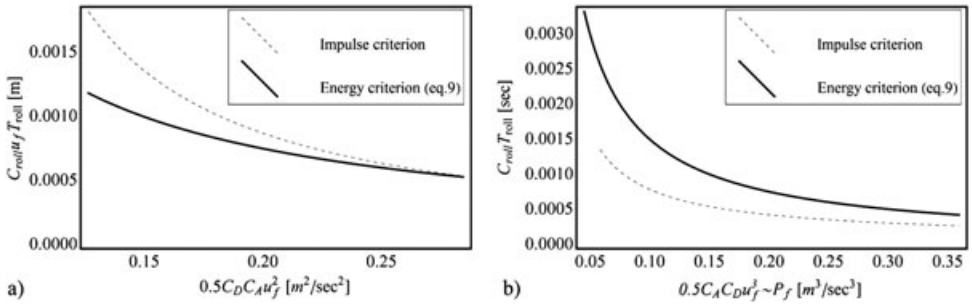

Figure 4. Illustration of the energy threshold for entrainment of a 12.6 mm particle in rolling mode by: (a) characteristic specific energy ($\sim u_f^2$) and length scale combinations, and (b) mean flow power (P_f) and duration ($C_{roll}T_{roll}$) combinations.

impulse required for particle entrainment in saltation mode [cf. equation (5) in *Valyrakis et al*., 2011, or equation (16) in *Valyrakis et al*., 2010]. A direct comparison of the two criteria may be performed, by plotting the threshold curve $I_{roll}\cdot u_p$ (dashed curve in Figures 4a and 4b). Compared to the energy criterion, $I_{roll}\cdot u_p$ overestimates the threshold for relatively low specific energy ($\sim u_f^2$), due to the linearization of the equations of motion solved to compute I_{roll}. This is in agreement with the findings of *Valyrakis et al.* [2010], who observed increasing error (excess impulse) for decreasing magnitude of the flow event ($F_D \sim u_f^2$). Thus, the energy criterion provides a more accurate representation of the threshold of entrainment by rolling.

[28] The wide distribution of hydrodynamic forcing on a grain [*Hofland and Battjes*, 2006; *Schmeeckle et al*., 2007] added to the variability of effects of its local configuration [*Fenton and Abbott*, 1977; *Chin and Chiew*, 1993; *Kirchner et al*., 1990; *Dey and Debnath*, 2000; *Gregoretti*, 2008; *Recking*, 2009] complicate the exact identification of a rolling threshold by traditional methods. However, the constancy of the proposed criterion along with its ability to account for all those diverse but physically relevant effects in a simple and yet intuitive manner demonstrate its versatility and appropriateness for predictive purposes.

4. Incipient Entrainment Experiments

4.1. Description of Setup and Experimental Process

[29] Incipient motion experiments are performed to obtain coupled data for the instantaneous stream-wise flow velocity upstream a fully exposed Teflon (specific gravity=2.3) spherical particle in addition to its entrainment record. The test section is located 14 m downstream from the inlet of the 20.5 m long and 0.6 m wide open channel to guarantee fully developed turbulent flow conditions. The sphere (12.7 mm diameter) rests on top of two layers of fully packed glass beads of the same size, forming a tetrahedral arrangement (Figure 5). The bed slope (α) remains fixed to 0.25% for all of the conducted experiments. The series of conducted experiments refer to near-threshold to low-mobility conditions. Thus, for accurate identification of the flow events as well as entrainment instances, noninterference techniques are used [*Diplas et al*., 2010].

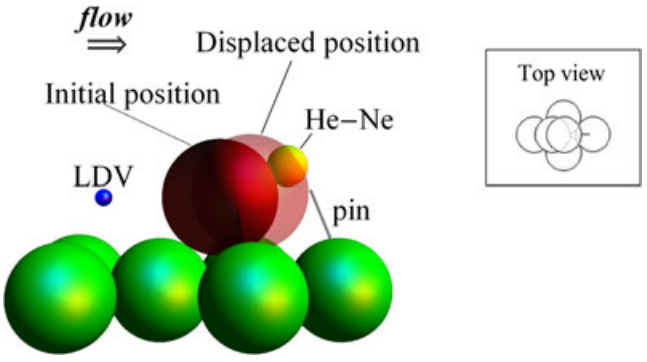

Figure 5. Sketch (side view) of the experimental setup (top view shown in the inset), illustrating the possible locations of the mobile particle and its local configuration with a retaining pin. The LDV measurement volume one particle diameter upstream the exposed sphere and the He-Ne laser beam partially targeting the particle are also shown.

[30] The motion of the mobile sphere is recorded via a particle tracking system composed of a photomultiplier tube and a low-power (25–30 mW) He-Ne laser source. As shown in Figure 5, the He-Ne laser beam is aligned to partially target the test particle. Calibration of the setup showed that the angular dislodgement of the targeted particle is a linear function of the signal intensity of the photomultiplier tube. A continuous series of entrainments is made possible due to a restraining pin located 1.5 mm downstream of the mobile sphere (Figure 5), which limits the maximum dislodgement of the grain to the displaced position. The grain will fall back to its initial position after the energetic flow structure has passed, without a need to interrupt the experiment to manually place the sphere back to its resting configuration.

[31] The time history of the stream-wise velocity component one diameter upstream of the particle and along its centerline [$u(t)$] is obtained by means of laser Doppler velocimetry (4 W Argon ion LDV) at an average sampling frequency of about 350 Hz (Figure 5). These measurements are obtained simultaneously with the displacement signal, using a multichannel signal processor. Using equation (1), the energetic events can be extracted from the time series of $P_f = f(u_f^3)$.

[32] A series of experiments are carried out, during which coupled measurements of flow intensity and particle response were recorded for different low-mobility flow conditions. All of these experiments refer to near-incipient motion conditions of about the same mean local velocity, u_{mean}, and dimensionless Shields bed shear stress, τ^*, whereas the rate of occurrence of energetic events, f_P, and rate of particle entrainment, f_E, changes more than an order of magnitude (Table 1). For each of the experimental runs, the flow conditions were stabilized to achieve a constant rate of mobile particle displacement, f_E, over long durations (about 2 hours). The 15 minute long, synchronized time series of flow power as a function of the cube of the recorded instantaneous stream-wise velocity component [u_f(t)] and grain angular displacement [θ(t)] are analyzed to examine the validity of the energy concept.

5. Results and Discussion

5.1. Trajectory Analysis of Rolling Particle

[33] In an effort to demonstrate the utility of the proposed criterion and its versatility in characterizing threshold conditions for a variety of flow event features, the dynamics of grain entrainment are analyzed for three representative cases of different duration, energy content, and energy

Table 1. Summary of Flow Characteristics for Incipient Entrainment Experiments

	u_{mean} (m/s)	τ^* (-)	f_P (events/s)	f_E (entrainment/s)
E1	0.248	0.007	2.23	0.147
E2	0.243	0.007	1.75	0.114
E3	0.238	0.006	1.33	0.051
E4	0.230	0.006	0.81	0.031
E5	0.218	0.005	0.33	0.002
E6	0.228	0.005	0.58	0.012
E7	0.227	0.005	0.48	0.008

transfer coefficient. Flow energy is transferred to the grain when the condition $u_f(t)>u_c(t)$ is satisfied, with $u_c(t)$ representing the history of the gravitational force component resisting the grain's displacement at any time instant, t:

$$u_c(t) = \sqrt{\frac{2\left(\rho_s-\rho_f\right)}{\rho_f C_D A} f_h mg \frac{\cos\theta(t)}{\sin(\theta(t)-\alpha)}} \tag{10}$$

where the hydrodynamic mass coefficient is given by $f_h=[\rho_s-\rho_f(1-C_m)]/(\rho_s-\rho_f)$, with C_m the added mass coefficient. For the drag coefficient, a constant value of $C_D=1$ is used here. Then the condition $u_f(t)>u_c(t)$ is similar to the condition $u_f(t)>u_c$ [cf. equation (4) in *Valyrakis et al.*, 2011], but with $u_c(t)$ changing as a function of the angular displacement [$\cos\theta(t)$]. This essentially lowers the down-crossing level (the threshold level defining when the event ceases), rendering the flow events detection scheme less sensitive to the fluctuation of $u_f(t)$. In a different case, a single flow event might be shown as a number of different trailing flow pulses, due to consecutive upcrossings and downcrossings from a constant u_c. Thus the above condition may better represent the energetic events that perform work on the particle. The magnitude of particle response (from twitches to energetic entrainment), as well as the total time required to achieve it (t_{tot}), depends on the rate and effectiveness of energy transfer and the duration of the flow event. Thus, it is expected that the dynamics of grain entrainment show a wide range of attributes, which are captured by the following examples.

[34] Several quantities of interest, such as the representation of the power of the resisting forces, $u_c^3(t)$, and the flow power [$u_f^3(t)$] (Figure 6), the net power transferred to the grain (Figure 7), and the work performed on it (Figure 8), are provided for three distinctive entrainment events. In particular, the power function, P_f, plotted in Figure 6, is the product of $u_c^3(t)$ or $u_f^3(t)$ with $0.5\rho_f C_D \pi R_m^2$. The net power function (Figure 7) is the product $\Sigma F\cdot u_p=[F_D\cdot\sin(\theta(t))-(W-B_f)\cos(\theta(t))]\cdot u_p$, whereas the mechanical work (Figure 8) is the sum of kinetic and potential energies of the particle, $W_{p,r}=(7/10)m_{tot}u_p{}^2+(W-B_f)\cos(\theta(t))$. The latter is obtained from the particle displacement signal.

[35] The first event is a short-lived but of significantly high magnitude flow event (Figure 6a). On the other extreme, the second flow event has longer duration but lower magnitude (Figure 6b). The third case lies in between, but compared to the first event has greater value of C_{eff} (Figure 6c). The figures include a short history of the above variables ranging from about 0.55 s before the instant of inception of motion (shown with the dashed vertical line) until the time the entrainment ceases when the retaining pin is reached. Beyond this location, [$\theta(t_{tot})$] grain entrainment is certain because the mean flow velocity becomes greater than the reduced critical level [$u_m>u_c(t_{tot})$].

[36] For the cases with relatively longer durations of particle entrainment, the particle may dislodge to positions of reduced resistance (e.g., dotted line in Figures 6b and 6c), which may effectively render smaller than initially required flow events capable of performing work on the particle to complete its entrainment. In most of the cases, the detected

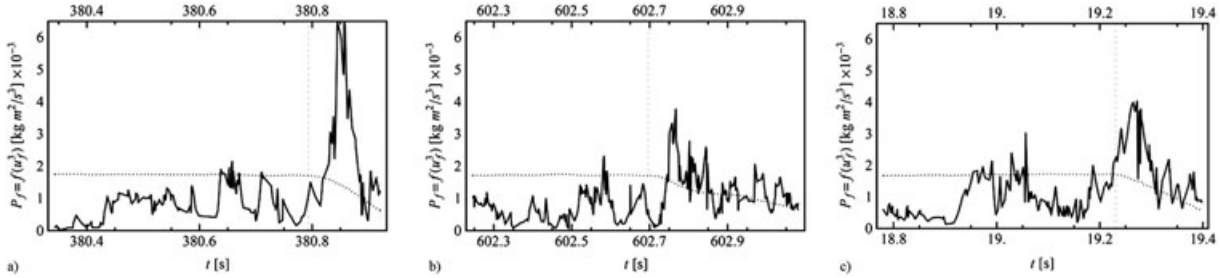

Figure 6. Representation of the available flow power and corresponding resistance level (dotted curve) for representative cases of particle entrainment: (a) relatively short flow event of high-energy content, (b) long duration of flow event and low-energy content, and (c) relatively high C_{eff}. Vertical dashed line shows the instant of initiation of entrainment.

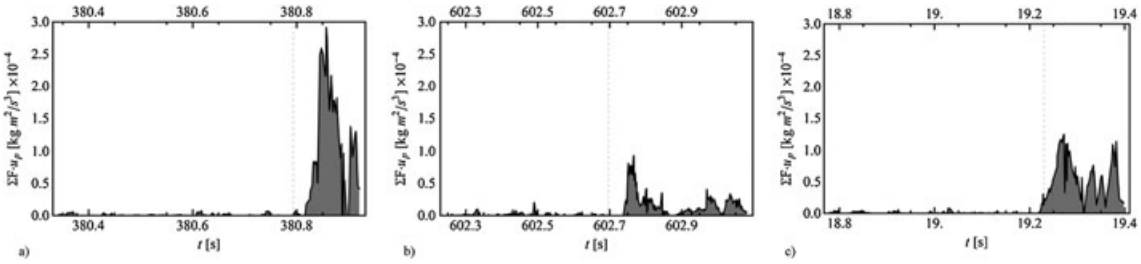

Figure 7. Representation of the net power transferred toward the grain's dislodgement (shaded area corresponds to the total offered energy) for representative cases of particle entrainment: (a) relatively short flow event of high-energy content, (b) long duration of flow event and low-energy content, and (c) representative case of relatively high C_{eff}. Vertical dashed line shows the instant of initiation of entrainment.

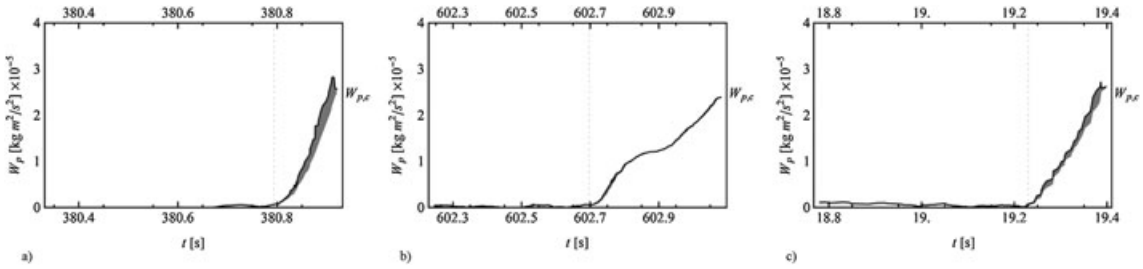

Figure 8. Representation of the history of the mechanical work performed on the particle until the critical level is reached for representative cases of particle entrainment: (a) relatively short duration of flow event and high specific energy, (b) long duration of flow event and low specific energy, and (c) representative case of relatively high C_{eff}. Vertical dashed line shows the instant of initiation of entrainment, and shaded area corresponds to the kinetic energy of the particle.

flow events on their own offer sufficient energy for complete grain entrainment. For those cases, highly peaking energetic flow events offer an energy surplus toward a stronger and faster grain response. When the flow events do not last enough to transfer sufficient energy, only a small displacement is initially possible (e.g., twitching motion). In these cases the particle is brought to a new position of reduced resistance. The lower the new threshold is, the higher the probability that a follow-up flow event may occur [*Celik et al*., 2010; *Valyrakis et al*., 2011]. In this manner, there is a good chance that a series of successive flow events (that otherwise would be ineffective) might provide the remaining energy required for completing the entrainment downstream, before it falls back in its resting pocket (Figure 6b). According to the above mechanism, a number of consecutive small peaked flow events may become effective in entraining the particle. Depending on the temporal separation of those peaks, the particle might undergo several phases during which particle energy increases or gets dissipated. In this case, particle entrainment is feasible only when the local energy budget of the particle (equal to the total energy offered from these flow events minus the overall dissipated energy) exceeds the critical energy level. The general energy criterion could then be extended to account for those cases i: $\Sigma W_{p,i}(t_{tot,i}) > W_{p,c}$.

[37] The instantaneous rate of transferred flow energy, $\Sigma F \cdot u_p$, is also proportional to the difference of the power functions of $u_f(t)$ and $u_c(t)$, with C_{roll} as a proportionality constant. This may be readily seen by comparing the events of Figure 7 with the corresponding events of Figure 6. Even though the magnitude of flow events following a peak event is relatively lower, the reduced resistance and increased particle velocity toward the end of movement may result in energy transfer rates between the flow events of comparable magnitude (Figure 7c).

[38] The integral of the rate of energy transfer from the instant of onset of movement until time $t < t_{tot}$ indicates the mechanical work performed on the particle. In the first case, the highly energetic flow event transfers additional energy above the critical level and at a high rate. As a result, the particle reaches the fully exposed position relatively fast, with an excess amount of kinetic energy $[W_p(t_{tot}) > W_{p,c}]$, which in the absence of the pin would possibly allow it to get transported several diameters downstream (Figure 8a). Quite the reverse holds for the second case, where the weak flow events barely manage to displace the grain until the final position (Figure 8b). Because of the low rate of energy transfer (Figure 7b), the critical energy level is reached at a relatively high t_{tot} (more than twice the mean).

5.2. Comparison of Experimental Data to Theoretical Predictions

[39] The energetic events are detected based on equation (1) and using the cube of the stream-wise velocity signal to parameterize the instantaneous flow power. Analysis of the synchronously obtained entrainment signal reveals whether each of the extracted flow events manages to completely dislodge the particle. The data points that manage to perform mechanical work and entrain the particle are shown in Figure 9 (solid circles). Also as shown in Figure 9, most of the detected energetic flow events that manage to fully entrain the particle fall above the energy threshold. For example, only 6% or 6 of 104 events, for run E1, fall below the threshold level defined by equation (9).

[40] The critical energy level should remain the same because the particle and its local arrangement are fixed for all of the performed experiments. The energy transfer coefficient may be defined considering that its product with the available energy content of each flow event should at least equal or exceed the minimum required work done on the particle for its dislodgement. As illustrated in Figure 9, as well as predicted from equation (9), the higher the value of the energy transport efficiency, the lower the required flow energy. Most of the flow events resulting in entrainment

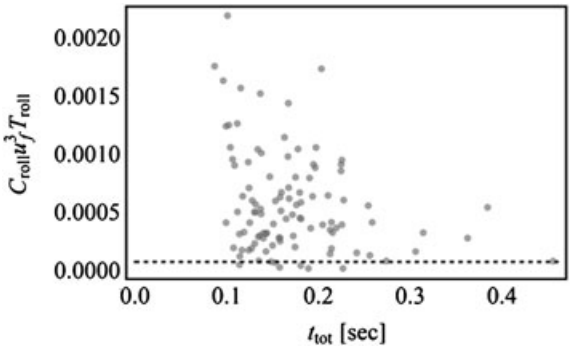

Figure 9. Plot of energy content of flow events ($C_{roll}u_f^3T_{roll}$) against the total duration for entrainment (t_{tot}), for experimental run E1, showing also the threshold energy level (dashed line) as predicted from equation (9).

have a C_{eff}, ranging from 0.04 to 0.10 (Figures 10 and 11). C_{eff} essentially describes how more effective a certain flow event is compared to another, due to effects not explicitly accounted for in the energy transfer equation (2). Such effects may be associated to the duration of the flow event, possible contributions of follow-up flow events, and the exact structure (velocity signature) of the flow event. For example, a relatively long near-critical flow event is observed to correspond to a low value of C_{eff}, whereas the positive contribution of a strong vertical velocity component may be associated with a high C_{eff} value.

[41] In the case of natural grains, C_{eff} would also integrate effects due to grain shape parameters (e.g., angularity, true sphericity, shape factor) and local grain microtopography features (orientation, protrusion). The implication is that different flow structures will have varying effectiveness in entraining a naturally shaped grain. Thus, for given flow conditions, the range of C_{eff} values is expected to be wider compared to the case of rounded particles examined in this study.

5.3. Characteristic Features of Energetic Events Resulting in Particle Entrainment

[42] As already discussed, the basis of the proposed energy concept is that the rate of occurrence, as well as the characteristics, of energetic events are associated with the rate of work done on sediment particles. The magnitude of the energetic flow events relative to the particle and local microtopography characteristics define the particle's stability or resistance to entrainment. For a particle saltating due to the action of extreme magnitude and short-lived hydrodynamic lift [*Smart and Habersack*, 2007], it is more intuitive to describe the supply of flow energy in terms of duration and mean flow power above a critical level [equation (1)]. Regarding the case of a grain rolling out of its resting pocket due to an impinging flow structure, it is physically sound to consider the flow energy density and its characteristic length scale as the relevant parameters.

[43] The distributions of these features characterizing the overall energy content of the flow events are shown in Figures 12 and 13. It is important to observe that the majority of flow events (more than 50%) resulting in dislodging of the particle have a characteristic length scale of the same order as the particle diameter, $2R_m$=12.7mm (Figure 12). About a quarter of the data points belonging in the entrainment region are associated to a horizontal length scale for the flow events ranging from two to three times the particle diameter. A significantly lower fraction of particle entrainment events occurs because of flow structures of size greater than four times the particle's diameter. Concerning the distribution of energy density, it may be readily observed that it varies over a relatively narrower range (about 50% compared to fivefold increase of the length scale). The synergetic action of those features may explain why a significant amount of work

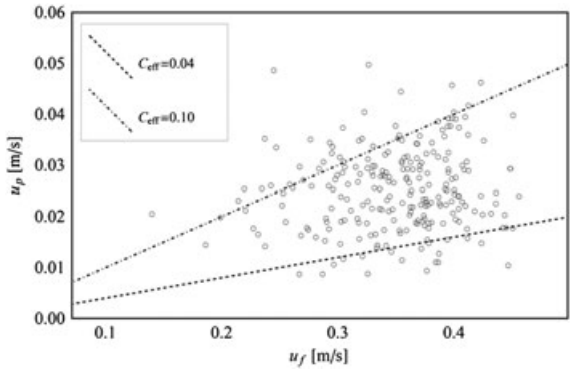

Figure 10. Relation between the mean velocity of the flow event and the resulting particle velocity (averaged over the duration of dislodgement).

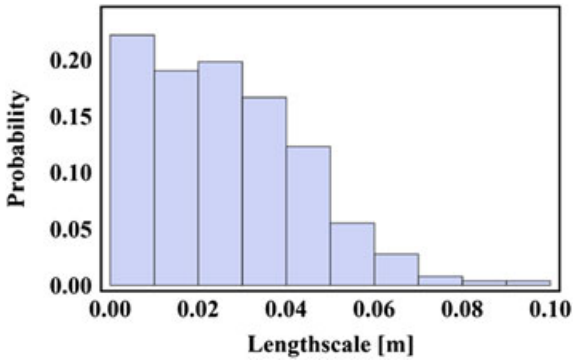

Figure 12. Probability distribution of the characteristic length scale of the flow events (for all experiments).

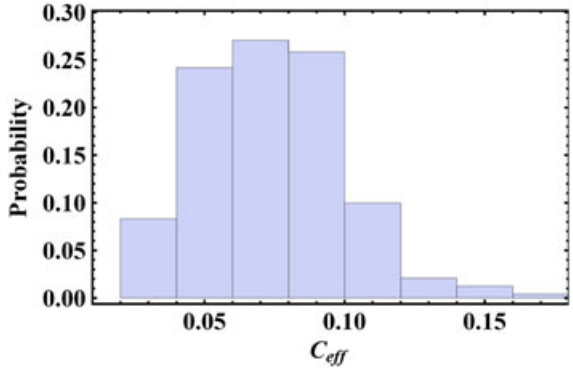

Figure 11. Distribution of the coefficient of energy transfer, C_{eff} (values from all experiments).

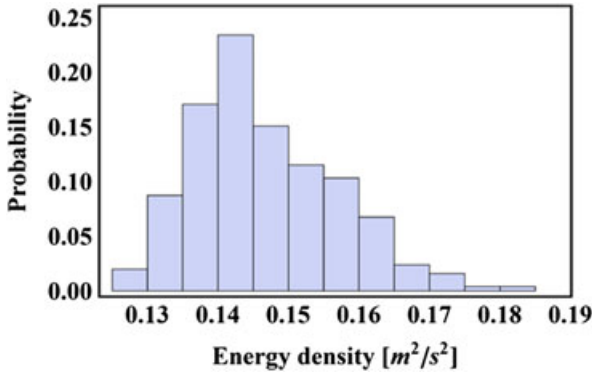

Figure 13. Probability distribution of the energy density of the flow events (for all experiments).

performed in transporting bed material or equivalently an increase in bed load may be observed in cases where an increase in organized coherent flow structures is present in the flow field even for about the same shear stress [*Shvidchenko and Pender*, 2001; *Sumer et al*., 2003]. This finding is consistent with the experimental results of Hofland *et al*. [2005], reporting sizes of sweeps structures ranging from 2 to 4 grain diameters in the stream-wise direction and 0.5 to 1 grain diameter in the stream normal direction. Plotting the bivariate distribution of the length scales and energy densities of the flow events, it can be readily observed that the longer event durations (high length scales) are associated with lower energy densities (Figure 14).

5.4. Comparison of Saltation and Rolling Thresholds

[44] Based on equation (2), a comparison of the minimum flow energy supplied for entrainment by saltation and rolling assuming the same order of magnitude of energy transport coefficients reveals that a greater amount of mechanical work is required for saltating grains. This may be readily illustrated by estimating the ratio of the two thresholds:

$$\frac{W_{p,roll}}{W_{p,salt}} = \frac{(1-\sin\theta_0)L_{arm}}{2R_m}, \tag{11}$$

which for moderate slopes and ratio of mobile to base particles greater than 0.2 is always less than unity. Then, according to equation (11), the saltation threshold is greater than the critical value for rolling. For the case of the incipient motion experiments, this ratio is 0.1. This implies that to observe particles being entrained by saltation, the magnitude of energy of the flow events has to exceed 10 times the critical level for rolling. However, the maximum flow energy observed for all experiments is close to fivefold the rolling threshold, which explains why rolling is the sole expected entrainment mode for the examined flow conditions. This remark is in qualitative agreement with the results reported in the literature [*Bagnold*, 1973; *Ling*, 1995; *Wu and Chou*, 2003].

5.5. Comparison of Energy and Impulse Criteria

[45] The impulse and energy criteria may be derived from the two fundamental formulations of equations of motion of classical mechanics, the Newtonian and Lagrangian, which are interconnected [e.g., *Yang*, 1992]. In practice, a direct link between the two concepts may be readily established assuming infinitesimally small displacements, Δx, over the duration (T) of application of the hydrodynamic force F (with F representing a mean force magnitude over T). Then the required mechanical work performed on the particle is $W_{p,c}=F\cdot\Delta x$, where $\Delta x=T\cdot u_p$ and u_p is the mean velocity of the particle over the duration T. Then equation (1) becomes: $I=F\cdot T=W_{p,c}/u_p$, or $W_{p,c}=I\cdot u_p$, which is the energy-impulse equation, essentially linking the two criteria.

[46] Beyond their direct interconnection and linkage with respect to their derivation from first principles, the impulse and energy concepts are physically sound and more appropriate compared to past traditional approaches, given the fluctuating nature of the applied hydrodynamic forces. They are compatible to the dynamic character of particle transport, by accounting for the temporal dimension of high-magnitude turbulent events. In accordance to many observations in the literature arguing for the intermittent and episodic nature of particle entrainment at near-threshold flow conditions, the impulse and energy criteria are threshold-based theories where only the randomly occurring high-magnitude events (in excess of a momentum, I_{cr}, or energy threshold, W_{cr}, respectively) may trigger particle entrainment. Thus, both approaches may be implemented using an appropriate stochastic modeling framework such as extreme value theory [*Valyrakis et al*., 2011].

6. Conclusions

[47] Herein a new criterion for identification of the incipient flow conditions is proposed, following an energy approach. The basis for its development relies on the concept that a portion of the available energy of sufficiently energetic flow events is dissipated in performing mechanical work on solid grains by mobilizing and transporting them downstream. It is hypothesized that only events imparting energy at a rate above a critical power level for a sufficiently long duration may mobilize coarse grains from the bed matrix. Equivalently, the product of energy content of flow events with their characteristic length scale has to exceed a critical energy level, which equals the work of the forces resisting movement.

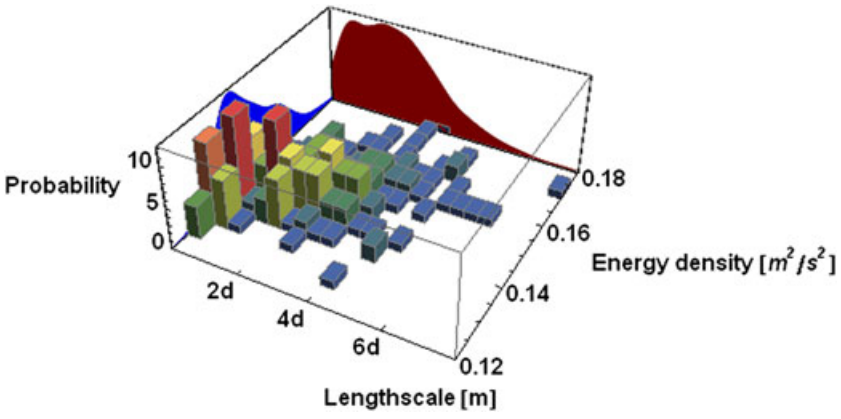

Figure 14. Plot of the bivariate density distribution of the energy density and characteristic length scale of the flow events (for all experiments).

[48] A theoretical framework for entrainment of spherical particles in saltation or rolling mode is developed using the energy balance equation, incorporating a coefficient to account for the efficiency of energy transfer. Equations defining the threshold energy curves are provided for both entrainment modes. In agreement with results reported in the literature, the limit for saltation is greater than for rolling.

[49] The validity of the concept is elucidated via a series of low-mobility experiments using nonintrusive equipment to accurately acquire synchronous measurements of the entrainment instances of an individual particle by rolling in addition to the flow events triggering them. The energetic flow structures are extracted based on a detection algorithm, and they are subsequently distinguished according to their impact on grain displacement. For appropriate values of the energy transport coefficient, the theoretically predicted threshold curves perform satisfactory in determining whether a flow event will dislodge the mobile particle.

[50] It is found that even though the energetic flow events exhibit a wide range of characteristic magnitude, the ability of the majority of the events to perform sufficient mechanical work on the coarse grain for entrainment is limited to only a small percentage of those having relatively high energy content.

Notation

α bed slope.
Δp_m mean pressure difference between the top and bottom of the particle for a flow event ($kg m^{-1} s^{-2}$).
θ_0 pivoting angle.
ν kinematic viscosity of medium (water) (m^2/s).
ρ_f density of the fluid (kg/m^3).
ρ_s density of the particle (kg/m^3).
τ_* dimensionless bed shear stress.
B_f buoyancy force ($kg \cdot m/s^2$).
C_D drag coefficient.
C_{eff} energy transfer coefficient.
C_p mean pressure coefficient.
C_{roll} coefficient for the energy transfer for a rolling particle.
C_{salt} coefficient for the energy transfer for a saltating particle.
$E_{f,i}$ available energy of flow event i ($kg \cdot m^2/s^2$).
$E_{f,r}$ energy of flow event resulting in particle entrainment by rolling ($kg \cdot m^2/s^2$).
$E_{f,s}$ energy of flow event resulting in particle entrainment by saltation ($kg \cdot m^2/s^2$).
F_{cr} critical force level ($kg \cdot m/s^2$).
F_D hydrodynamic drag force ($kg \cdot m/s^2$).
F_L hydrodynamic lift force ($kg \cdot m/s^2$).
f_E mean rate of particle entrainment.
f_I mean rate of occurrence of impulses.
f_h hydrodynamic mass coefficient.
g gravitational acceleration (m/s^2).
I_{cr} critical impulse level ($kg \cdot m/s$).
L_{arm} lever arm (m).
P_f instantaneous local power of the flow.
R_* boundary Reynolds number.
T_{salt} duration of flow event (for entrainment by saltation) (s).
T_{roll} duration of flow event (for entrainment by rolling) (s).
t_i time instance when event i occurs (s).
u_* shear velocity (m/s).
u_{cr} critical flow velocity (m/s).
u_f local flow velocity averaged over the duration of the flow event (m/s).
$u_f(t)$ instantaneous local flow velocity (m/s).
u_m time-averaged flow velocity (m/s).
V volume of the particle (m^3).
W weight of the particle (kg).
W_p work done on the particle ($kg \cdot m^2/s^2$).
$W_{p,cr}$ mechanical energy required for complete particle entrainment ($kg \cdot m^2/s^2$).
$W_{p,r}$ mechanical energy required for complete particle entrainment by rolling ($kg \cdot m^2/s^2$).
$W_{p,s}$ mechanical energy required for complete particle entrainment by saltation ($kg \cdot m^2/s^2$).

[51] **Acknowledgments.** The support of the National Science Foundation (EAR-0439663, EAR-0738759, and CBET-1033196) and Army Research Office is gratefully acknowledged.

References

Apperley, L. W., and A. J. Raudkivi (1989), The entrainment of sediments by the turbulent flow of water, *Hydrobiologia*, *176/177*, 39–49.

Bagnold, R. A. (1956), The flow of cohesionless grains in fluids, *Philos. Trans. R. Soc. London A*, *249*(964), 235–297.

Bagnold, R. A. (1966), An approach of sediment transport model from general physics, *U.S. Geol. Survey Prof. Paper 422-I*.

Bagnold, R. A. (1973), The nature of saltation and of 'bed-load' transport in water, *Philos. Trans. R. Soc. London A*, *332*(1591), 473–504, doi:10.1098/rspa.1973.0038.

Bagnold, R. A. (1977), Bed load transport by natural rivers, *Water Resour. Res.*, *13*, 303–312.

Bagnold, R. A. (1980), An empirical correlation of bedload transport rates in flumes and natural rivers, *Philos. Trans. R. Soc. London A*, *372*(1751), 453–473.

Bagnold, R. A. (1986), Transport of solids by natural water flow: Evidence for a worldwide correlation, *Philos. Trans. R. Soc. London A*, *405*(1829), 369–374.

Benedict, B. A., and B. A. Christensen (1972), Hydrodynamic lift on a stream bed, in Sedimentation, Symp. to Honor Prof. H. A. Einstein, edited by H. W. Shen, pp. 5.1–5.17, Water Resources Publication, Littleton, Colo.

Bettess, R. (1984), Initiation of sediment transport in gravel streams, *Proc. Inst. Civil Eng.*, *77*, 79–88.

Buffington, J. M., and D. R. Montgomery (1997), A systematic analysis of eight decades of incipient motion studies, with special reference to gravel-bedded rivers, *Water Resour. Res.*, *33*(8), 1993–2029.

Celik, A. O., P. Diplas, C. L. Dancey, and M. Valyrakis (2010), Impulse and particle dislodgement under turbulent flow conditions, *Phys. Fluids*, *22*(4), 046601.

Cheng, N.-S., and Y. M. Chiew (1998), Pickup probability for sediment entrainment, *J. Hydraul. Eng.*, *124*(2), 232–235.

Chepil, W. (1958), The use of evenly spaced hemispheres to evaluate aerodynamic forces on soil surfaces. *Eos Trans. AGU*, *39*, 397–403.

Chin, C. O., and Y. M. Chiew (1993), Effect of bed surface structure on spherical particle stability, *J. Waterway Port. Coastal Ocean Eng.*, *119*(3), 231–242.

Dey, S., and K. Debnath (2000), Influence of streamwise bed slope on sediment threshold under stream flow, *J. Irrigat. Drain. Eng.*, *126*(4), 255–263.

Diplas, P., C. L. Dancey, A. O. Celik, M. Valyrakis, K. Greer, and T. Akar (2008), The role of impulse on the initiation of particle movement under turbulent flow conditions, *Science*, *322*(5902), 717–720, doi:10.1126/science.1158954.

Diplas, P., A. O. Celik, C. L. Dancey, and M. Valyrakis (2010), Non-intrusive method for detecting particle movement characteristics near threshold flow conditions, *J. Irrig. Drain. Eng.*, *136*(11), 774–780.

Dwivedi, A., B. W. Melville, A. Y. Shamseldin, and T. K. Guha (2010), Drag force on a sediment particle from point velocity measurements: A spectral approach, *Water Resour. Res.*, *46*, W10529, doi:10.1029/2009WR008643.

Dwivedi, A., B.W. Melville, A. Y. Shamseldin, and T. K. Guha (2011a), Analysis of hydrodynamic lift on a bed sediment particle, *J. Geophys. Res.*, *116*, F02015, doi:10.1029/2009JF001584.

Dwivedi, A., B. W. Melville, A. Y. Shamseldin, and T. K. Guha (2011b), Flow structures and hydrodynamic force during sediment entrainment, *Water Resour. Res.*, *47*, W01509, doi:10.1029/2010WR009089.

Einstein, H. A., and E.-S. A. El-Samni (1949), Hydrodynamic forces on a rough wall, *Rev. Mod. Phys.*, *21*(3), 520–527.

Fenton, J. D., and J. E. Abbott (1977), Initial movement of grains on a stream bed: The effect of relative protrusion, *Proc. R. Soc. London A*, *352*(1671), 523–537.

Gilbert, G. K. (1914), The transportation of debris by running water, *U.S. Geol. Surv. Prof. Paper*, *86*, 263.

Gregoretti, C. (2008), Inception sediment transport relationship at high slopes, *J. Hydraul. Eng*, *11*(134), 1620–1629.

Hjulström, F. (1939), Transportation of debris by moving water, in Recent Marine Sediments, edited by P. D. Trask, pp. 5–31, American Association of Petroleum Geologists, Tulsa, Okla.

Hofland, B., and J. Battjes (2006), Probability density function of instantaneous drag forces and shear stresses on a bed, *J. Hydraul. Eng.*, *132*(11), 1169–1175.

Hofland, B., R. Booij, and J. Battjes (2005), Measurement of fluctuating pressures on coarse bed material, *J. Hydraul. Engrg.*, *131*(9), 770–781.

James, C. S. (1990), Prediction of entrainment conditions for nonuniform, noncohesive sediments, *J. Hydraul. Res.*, *28*(1), 25–41.

Jeffreys, H. (1929), On the transportation of sediment by streams, *Proc. Cambridge Philos. Soc.*, *25*, 272–276.

Kirchner, J. W., W. E. Dietrich, F. Iseya, and H. Ikeda (1990), The variability of critical shear stress, friction angle, and grain protrusion in water-worked sediments, *Sedimentology*, *37*(4), 647–672.

Knapp, R. T. (1938), Energy balance in stream flows carrying suspended load, *Am. Geophys. Union Trans.*, 501–505.

Komar, P. D., and Z. Li (1988), Applications of grain pivoting and sliding analyses to selective entrainment of gravel and to flow competence evaluations, *Sedimentology*, *35*, 681–695.

Lavelle, J. W., and H. O. Mofjeld (1987), Do critical stresses for incipient motion and erosion really exist?, *J. Hydraul. Eng. 113*(3), 370–385.

Ling, C.-H. (1995), Criteria for incipient motion of spherical sediment particles, *J. Hydraul. Eng.*, *121*(6), 472–478.

Miller, M. C., I. N. McCave, and P. D. Komar (1977), Threshold of sediment motion under unidirectional currents, *Sedimentology*, *24*, 507–527.

Nino, Y., F. Lopez, and M. Garcia (2003), Threshold for particle entrainment into suspension, *Sedimentology*, *50*, 247–263.

Paintal, A. S. (1971), Concept of critical shear stress in loose boundary open channels, *J. Hydraul. Res.*, *9*(1), 91–113.

Papanicolaou, A., P. Diplas, C. L. Dancey, and M. Balakrishnan (2001), Surface roughness effects in near-bed turbulence: Implications to sediment entrainment, *J. Eng. Mech.*, *127*(3), 211–218.

Papanicolaou, A. N., P. Diplas, N. Evaggelopoulos, and S. Fotopoulos (2002), Stochastic incipient motion criterion for spheres under various bed packing conditions, *J. Hydraul. Eng.*, *128*(4), 369–380.

Paphitis, D., M. B. Collins, L. A. Nash, and S. Wallbridge (2002), Settling velocities and entrainment thresholds of biogenic sands (shell fragments) under unidirectional flows, *Sedimentology*, *49*, 211–225.

Recking, A. (2009), Theoretical development on the effects of changing flow hydraulics on incipient bed load motion. *Water Resour. Res.*, *45*, W04401, doi:10.1029/2008WR006826.

Rubey, W. W. (1933), Equilibrium conditions in debris-laden streams, *Am. Geophys. Union Trans., 14th Ann. Meeting*, U.S. Geological Survey, Washington, D.C.

Schmeeckle, M. W., J. M. Nelson, and R. L. Shreve (2007), Forces on stationary particles in near-bed turbulent flows, *J. Geophys. Res.*, *112*, F02003, doi:10.1029/2006JF000536.

Shields, A. (1936), Application of similarity principles and turbulence research to bed-load movement, Rep., No. 167, California Institute of Technology, Pasadena, Calif.

Shvidchenko, A. B., and G. Pender (2000), Flume study of the effect of relative depth on the incipient motion of coarse uniform sediments, *Water Resour. Res.*, *36*(2), 619–628.

Shvidchenko, A. B., and G. Pender (2001), Macroturbulent structure of open-channel flow over gravel beds, *Water Resour. Res.*, *37*(3), 709–719.

Smart, G. M., and H. M. Habersack (2007), Pressure fluctuations and gravel entrainment in rivers, *J. Hydraul. Res.*, *45*(5), 661–673.

Sumer, B. M., L. H. C. Chua, N.-S. Cheng, and J. Fredsoe (2003), Influence of turbulence on bed load sediment transport, *J. Hydraul. Eng.*, *129*(8), 585–596.

Sutherland, A. J. (1967), Proposed mechanism for sediment entrainment by turbulent flows, *J. Geophys. Res.*, *72*(24), 6183–6194.

Valyrakis, M., P. Diplas, C. L. Dancey, K. Greer, and A. O. Celik (2010), The role of instantaneous force magnitude and duration on particle entrainment, *J. Geophys. Res.*, *115*, 1–18, doi:10.1029/2008JF001247.

Valyrakis, M., P. Diplas, and C. L. Dancey (2011), Entrainment of coarse grains in turbulent flows: an Extreme Value Theory approach, *Water Resour. Res.*, *47*, W09512, doi:10.1029/2010WR010236.

Vollmer, S., and M. G. Kleinhans (2007), Predicting incipient motion, including the effect of turbulent pressure fluctuations in the bed, *Water Resour. Res.*, *43*, W05410, doi:10.1029/2006WR004919.

White, C. M. (1940), The equilibrium of grains on the bed of a stream, *Proc. R. Soc. London A*, *174*(958), 322–338.

Wu, F.-C., and Y.-J. Chou (2003), Rolling and lifting probabilities for sediment entrainment, *J. Hydraul. Eng.*, *129*(2), 110–119.

Wu, F.-C., and Y.-C. Lin (2002), Pickup probability of sediment under Log-Normal velocity distribution, *J. Hydraul. Eng.*, *128*(4), 438–442.

Wu, F.-C., and K.-H. Yang (2004), Entrainment probabilities of mixed-size sediment incorporating near-bed coherent flow structures, *J. Hydraul. Eng.*, *130*(12), 1187–1197.

Yang, C. T. (1972), Unit stream power and sediment transport, *J. Hydraul. Div.*, *98*, 1804–1826.

Yang, C. T. (1979), Unit stream power equations for total load, *J. Hydrol.*, *40*, 123–138.

Yang, C. T. (1992), Force, energy, entropy, and energy dissipation rate. Entropy and Energy Dissipation in Water Resources, edited by V. P. Sing and M. Fiorentino, Kluwer Academic Publisher, Netherlands, 63–89.

Yang, C. T., and A. Molinas (1982), Sediment transport and unit stream power function, *J. Hydraul. Div.*, *108*(HY6), 774–793.

Yang, C. T., and Stall, J. B. (1976), Applicability of unit stream power equation, *J. Hydraul. Div.*, *102*(HY5), 559–568.

Zanke, U. C. E. (2003), On the influence of turbulence on the initiation of sediment motion, *Int. J. Sed. Res.*, *18*(1), 17–31.